Current Biology 25, 218–224, January 19, 2015 ©2015 Elsevier Ltd All rights reserved http://dx.doi.org/10.1016/j.cub.2014.11.017

Report

Dynamic Visualization of α-Catenin Reveals Rapid, Reversible Conformation Switching between Tension States

Tae-Jin Kim,[1] Shuai Zheng,[2] Jie Sun,[3] Ismaeel Muhamed,[4] Jun Wu,[5] Lei Lei,[6] Xinyu Kong,[4] Deborah E. Leckband,[2,4,5,6,7,8,*] and Yingxiao Wang[1,2,3,6,8,9,*]

[1]Neuroscience Program

[2]Department of Bioengineering and Beckman Institute for Advanced Science and Technology

[3]Department of Integrative and Molecular Physiology

[4]Department of Biochemistry

[5]Department of Chemical and Biomolecular Engineering

[6]Center for Biophysics and Computational Biology

[7]Department of Chemistry

[8]Institute for Genomic Biology

University of Illinois at Urbana-Champaign, Urbana, IL 61801, USA

[9]Department of Bioengineering and Institute of Engineering in Medicine, University of California, San Diego, La Jolla, CA 92093, USA

Summary

The cytosolic protein α-catenin is a postulated force transducer at cadherin complexes [1]. The demonstration of force activation, identification of consequent downstream events in live cells, and development of tools to study these dynamic processes in living cells are central to elucidating the role of α-catenin in cellular mechanics and tissue function [2–10]. Here we demonstrate that α-catenin is a force-activatable mechanotransducer at cell-cell junctions by using an engineered α-catenin conformation sensor based on fluorescence resonance energy transfer (FRET). This sensor reconstitutes α-catenin-dependent functions in α-catenin-depleted cells and recapitulates the behavior of the endogenous protein. Dynamic imaging of cells expressing the sensor demonstrated that α-catenin undergoes immediate, reversible conformation switching in direct response to different mechanical perturbations of cadherin adhesions. Combined magnetic twisting cytometry with dynamic FRET imaging [11] revealed rapid, local conformation switching upon the mechanical stimulation of specific cadherin bonds. At acutely stretched cell-cell junctions, the immediate, reversible conformation change further reveals that α-catenin behaves like an elastic spring in series with cadherin and actin. The force-dependent recruitment of vinculin—a principal α-catenin effector—to junctions requires the vinculin binding site of the α-catenin sensor [1, 12–16]. In cells, the relative rates of force-dependent α-catenin conformation switching and vinculin recruitment reveal that α-catenin activation and vinculin recruitment occur sequentially, rather than in a concerted process, with vinculin accumulation being significantly slower. This engineered α-catenin sensor revealed that α-catenin is a reversible, stretch-activatable sensor that mechanically links cadherin complexes and actin and is an indispensable player in cadherin-specific mechanotransduction at intercellular junctions.

*Correspondence: leckband@illinois.edu (D.E.L.), yiw015@eng.ucsd.edu (Y.W.)

Results and Discussion

α-Catenin FRET Sensor Localizes to Intercellular Junctions and Restores α-Catenin-Dependent Functions in α-Catenin-Depleted Cells

We generated an α-catenin conformation sensor by inserting the fluorescent proteins ECFP and YPet into flexible linkers flanking the central, proposed force-sensing α-catenin module (domains D2–D4; Figure 1A). Western blots (Figure S1A available online) and fluorescence images (Figure S1B) verified the sensor expression and localization in transfected, α-catenin knockdown MDCK (MDCK KD) and in MDCK WT (wild-type) cells (Figure S1B). In western blots, the faint sensor band relative to endogenous α-catenin (Figure S1A) is attributed to the low sensor transfection efficiency. The biosensor localizes to intercellular junctions when expressed in either MDCK WT or MDCK KD cells, and it colocalizes with endogenous α-catenin (Figure S1B). The sensor similarly localized to junctions between transfected, α-catenin-deficient R2/7 cells (see Figures 1C and S1E).

The sensor is overexpressed in DLD1 and MDCK epithelial cells, but prior findings demonstrated that α-catenin-GFP overexpression in DLD1-R2/7 cells [15, 16] or in MDCK KD cells [16] did not affect cadherin-based mechanotransduction, vinculin and actin recruitment, or traction force generation [16]. Nor did cytosolic α-catenin depletion alter cadherin-based mechanotransduction [16].

The sensor expression restored α-catenin-dependent adhesive functions in α-catenin-deficient MDCK KD and DLD1-R2/7 cells. A signature of force transducers at cell adhesions is their ability to alter receptor-mediated spreading and traction force generation in response to substrate rigidity (Figure S1C) [16–18]. The sensor expression restored traction forces exerted by MDCK KD cells to MDCK WT levels (Figure S1D). Traction measurements were conducted in medium containing 0.5% FBS and the anti-α_v and anti-β_6 integrin antibodies GOH3 and AIIB2 in order to block integrin interference.

Cells exert greater traction forces on E-cadherin adhesions on rigid versus soft substrates [16, 17]. According to the sensor design (Figure 1A), the increased tension on cadherin adhesions would stretch α-catenin, separate YPet from ECFP, and decrease the fluorescence resonance energy transfer (FRET)/ECFP ratio. Consistent with a tension-dependent change in conformation, the basal FRET/ECFP ratios measured with DLD1-R2/7 cells expressing the α-catenin sensor were lower in cells adhered to more rigid (40 kPa modulus) E-cadherin-coated gels than in cells on softer gels (0.6 kPa modulus; Figures S1E and S1F). Together, these findings demonstrate that the engineered α-catenin FRET sensor localizes to intercellular junctions and rescues α-catenin-dependent adhesion, traction generation, and rigidity sensing at E-cadherin adhesions.

Altered Junctional Tension Triggers α-Catenin Conformation Switching

Altered physiological levels of tension across cadherin junctions were predicted to induce corresponding changes in dynamic FRET signals at different subcellular locations and

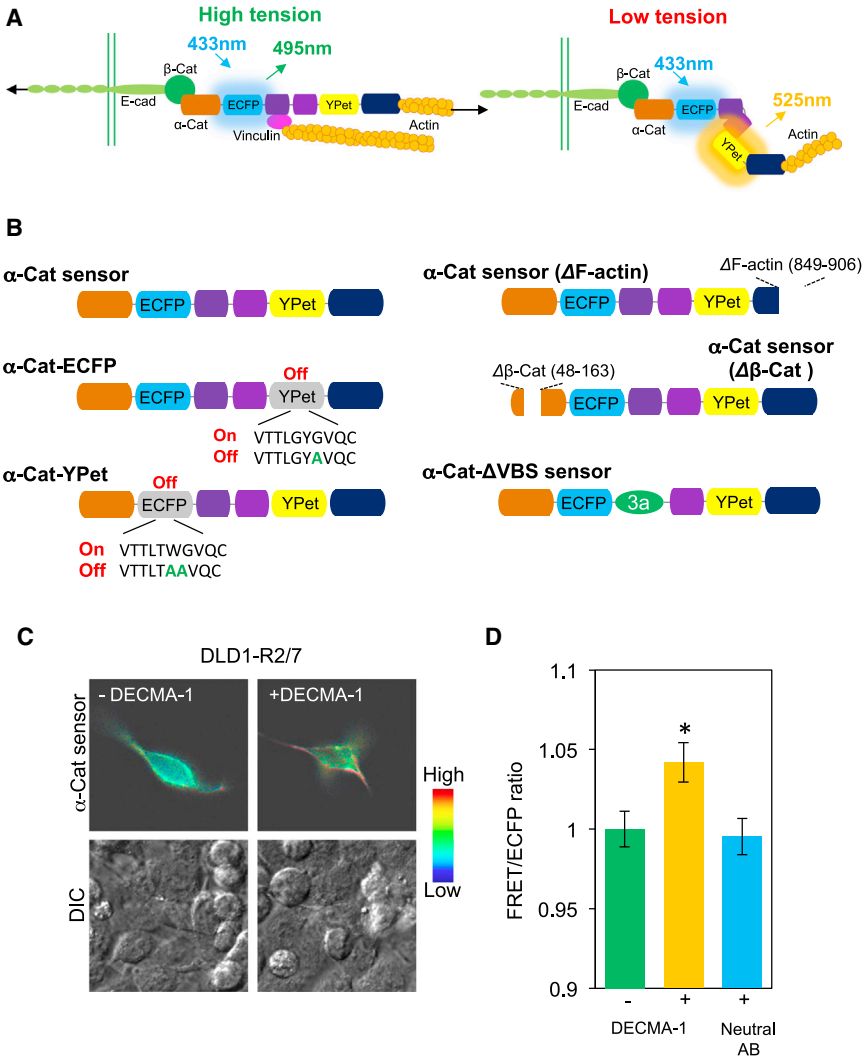

Figure 1. Design and Characterization of the FRET-Based α-Catenin Conformation Sensor

(A) Schematic of the postulated mechanism underlying α-catenin tension sensing. In this mechanism, high tension between cadherin/catenin adhesive complexes and F-actin induces a conformation change that would separate ECFP and YPet to reduce the FRET/ECFP ratio (left). Under low tension (for example, inactivated E-cadherin or actin disruption), the close fluorophores would increase the FRET/ECFP ratio (right).

(B) α-catenin sensor and mutants used in this study. In the wild-type sensor, two fluorescent proteins, ECFP and YPet, were inserted within flexible linker regions flanking the central force-sensitive region (domains D2–D4; purple). The orange and dark-blue domains are the β-catenin (D1) and the F-actin (D5) binding domains. Sensor variants include the fluorophore mutants α-Cat-ECFP and α-Cat-YPet, truncation mutants lacking F-actin (ΔF-actin) or β-catenin (Δβ-Cat) binding regions, and the α-Cat-ΔVBS mutant, which lacks the vinculin binding site.

(C) FRET/ECFP (top) and differential interference contrast (DIC; bottom) images of DLD1-R2/7 cells transfected with the sensor, before (left) and after (right) treatment with 50 μg/ml DECMA-1 antibody.

(D) Bar graph quantifying the relative impact of blocking DECMA-1 and neutral antibody treatment on the FRET/ECFP ratio at transfected DLD1-R2/7 cell junctions compared to untreated cells (n = 43–61; *p < 0.05). Error bars represent the SEM.

See also Figures S1, S2, and S4.

would allow the mapping of spatiotemporal activation patterns of α-catenin in cells. Three methods were used to disrupt mechanical coupling between cadherin bonds and F-actin (Figures 1C, 1D, and S2). Both E-cadherin-blocking antibody DECMA-1 (Figures 1C and 1D) [19] and removal of Ca^{2+} (Figures S2A and S2B) inactivate cadherin adhesion and lower intercellular tension [20]. Actin disruption with cytochalasin D (CytoD; Figures S2C–S2F) also destabilizes junctions and reduces tension [20, 21].

The observed increase in the FRET/ECFP ratio at regions of interest (ROIs) at cell junctions after junction disruption with inactivating antibody (Figures 1C and 1D) indicates a corresponding switch to the relaxed sensor conformation (Figure 1A, right). Results with a neutral, anti-E-cadherin antibody confirmed that cadherin inactivation caused the FRET/ECFP change (Figure 1D). At physiological Ca^{2+} concentrations (2 mM), the average FRET/ECFP ratio in ROIs at junctions between DLD1-R2/7 cells expressing the sensor was lower than between cells after Ca^{2+} removal (Figures S2A and S2B). The overall signal increase was complete within 2 min of Ca^{2+} removal and occurred well before the appearance of visible intercellular gaps. In studies with MDCK KD cells expressing the sensor, calcium removal also increased the FRET/ECFP ratio from 1.74 ± 0.03 to 2.04 ± 0.04 (n = 11, p < 0.01; data not shown).

Actin disruption with CytoD increased the FRET/ECFP ratio by ~7% relative to untreated DLD1-R2/7 cells (Figures S2C and S2D). With transfected MDCK KD cells expressing the sensor, CytoD treatment similarly increased the FRET/ECFP ratio at junctions from 1.67 ± 0.03 to 1.78 ± 0.04 (n = 14, p < 0.01; data not shown). This visualized tension-dependent conformation change occurred in the presence of endogenous α-catenin. At junctions between transfected MDCK WT cells, the FRET/ECFP ratio increased after CytoD treatment (Figures S2E and S2F). Changes in the cytosolic FRET/ECFP ratios were negligible (Figure S2F).

The tension-dependent conformation switch does not require the vinculin binding site (VBS), which is required for vinculin recruitment and local cytoskeletal remodeling [1, 9, 14, 16]. The α-Cat-ΔVBS-sensor, in which the VBS was replaced with the homologous vinculin sequence [1, 15, 16] (Figure 1B), retained the F-actin and β-catenin binding sites and localized to junctions (Figure S3A). CytoD treatment increased the FRET/ECFP ratio in DLD1-R2/7 cells expressing this mutant sensor, demonstrating that the vinculin site is not required for force-dependent conformation switching (Figures S3A and S3B).

Cytosolic α-Catenin Dimers Do Not Contribute to Tension-Dependent FRET Changes

To test whether dimers of the cytosolic α-catenin sensor[22] contribute to changes in force-dependent FRET/ECFP ratios, we engineered control constructs with point mutations

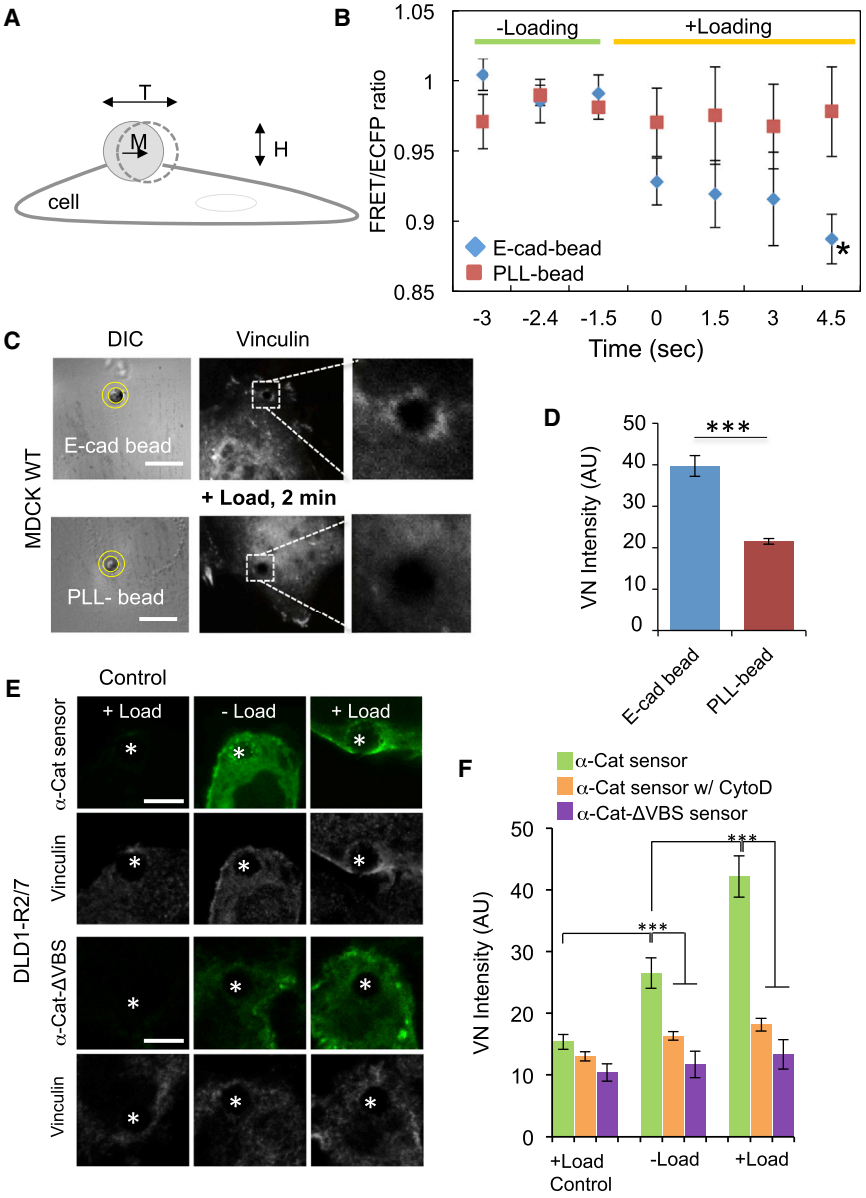

Figure 2. Acute Mechanical Perturbation of E-Cadherin Receptors Triggers Immediate α-Catenin Conformation Switching and Vinculin Recruitment

(A) Schematic of the magnetic twisting cytometry experiment. Ligand-coated ferromagnetic beads with a magnetic moment (M) are subjected to an orthogonal, oscillating field (H), which generates a torque (T) on the bead. The torque causes bead displacement, the amplitude of which is proportional to the bead-cell junction viscoelasticity.

(B) FRET/ECFP change in a ROI (yellow circles in C) around the E-cadherin-Fc- or PLL-coated beads bound to MDCK WT cells expressing the sensor (E-cadherin-Fc bead [n = 8] versus control PLL-bead [n = 4], *p < 0.05).

(C) DIC and vinculin immunofluorescence images of MDCK WT cells after 2 min of twisting beads bound to the apical surfaces. Images on the right were cropped and enlarged from the boxed regions of the original images. The DIC images indicate the ROI (yellow circles) used to quantify the distribution of vinculin at bead-cell junctions. Scale bars, 10 μm.

(D) Bar graph comparing the average vinculin accumulation (arbitrary units, AU) at E-cadherin beads versus control PLL beads on sensor-transfected MDCK WT cells after 2 min of loading (n = 21–24; ***p < 0.001).

(E) Sensor (green) and vinculin (gray) distributions at E-cadherin beads on DLD1-R2/7 cells expressing the WT α-Cat sensor (top) or the α-Cat-ΔVBS sensor (bottom). The white asterisk denotes the bead position. Scale bars, 5 μm. The left-hand panels show controls with nontransfected cells after loading. The center and right-hand panels show sensor and vinculin localization before and after loading.

(F) Bar graph comparing vinculin recruitment to E-cadherin beads on DLD1-R2/7 cells in (E) with or without force loading (n = 28–36; ***p < 0.001). CytoD treatment significantly reduced vinculin recruitment to E-cadherin beads in cells expressing the WT α-Cat sensor (n = 24–36).

Error bars (B), (D), and (F) indicate the SEM. See also Figure S3.

that quenched either ECFP or the YPet fluorescence (Figure 1B). The 67G>A substitution in YPet in the "α-catenin-ECFP" construct quenched YPet fluorescence, and the double mutant 66W>A, 67G>A in ECFP quenched ECFP fluorescence in the "α-catenin-YPet" construct [23, 24]. In both cases, the second fluorophore and the α-catenin core were unaffected (Figure S4A), and both mutants localized to junctions.

In MDCK WT cells cotransfected with both fluorophore mutants, CytoD treatment did not detectably alter the cytosolic or junctional FRET/ECFP ratio (Figures S4B and S4C). By comparison, the FRET/ECFP ratio in ROIs between MDCK WT cells expressing the WT α-Cat sensor increased by ~4% after actin disruption (Figures S4B and S4C). In MDCK WT cells expressing the WT α-Cat sensor, FRET/ECFP ratios in ROIs at junctions versus the cytosol also confirmed that cytosolic dimers do not undergo tension-dependent conformation changes (Figure S2F).

Cadherin-Specific Receptor Loading Triggers an Immediate α-Catenin Conformation Switch with Consequent Vinculin Recruitment

Cadherin-based mechanotransduction has been investigated by dynamic twisting of E-cadherin-coated ferromagnetic beads bound to E-cadherin receptors at the cell surface (Figure 2A) [16, 21, 25]. Combined magnetic twisting cytometry (MTC) and dynamic fluorescence imaging established spatiotemporal correlations between dynamic E-cadherin loading, α-catenin conformation switching, and vinculin recruitment. Prior to twisting of E-cadherin-Fc-coated beads attached to transiently transfected MDCK WT cells, the FRET/ECFP ratio in the ROI surrounding the beads (Figure 2C) was stable, but it decreased after bond shear (Figure 2B). The decreasing trend in the FRET/ECFP ratio was apparent within 1.5 s of data acquisition, and the difference was statistically significant at 4.5 s. Subsequent fluorescent images were acquired every 0.5 s, although Figure 2B reports the FRET/ECFP ratios at

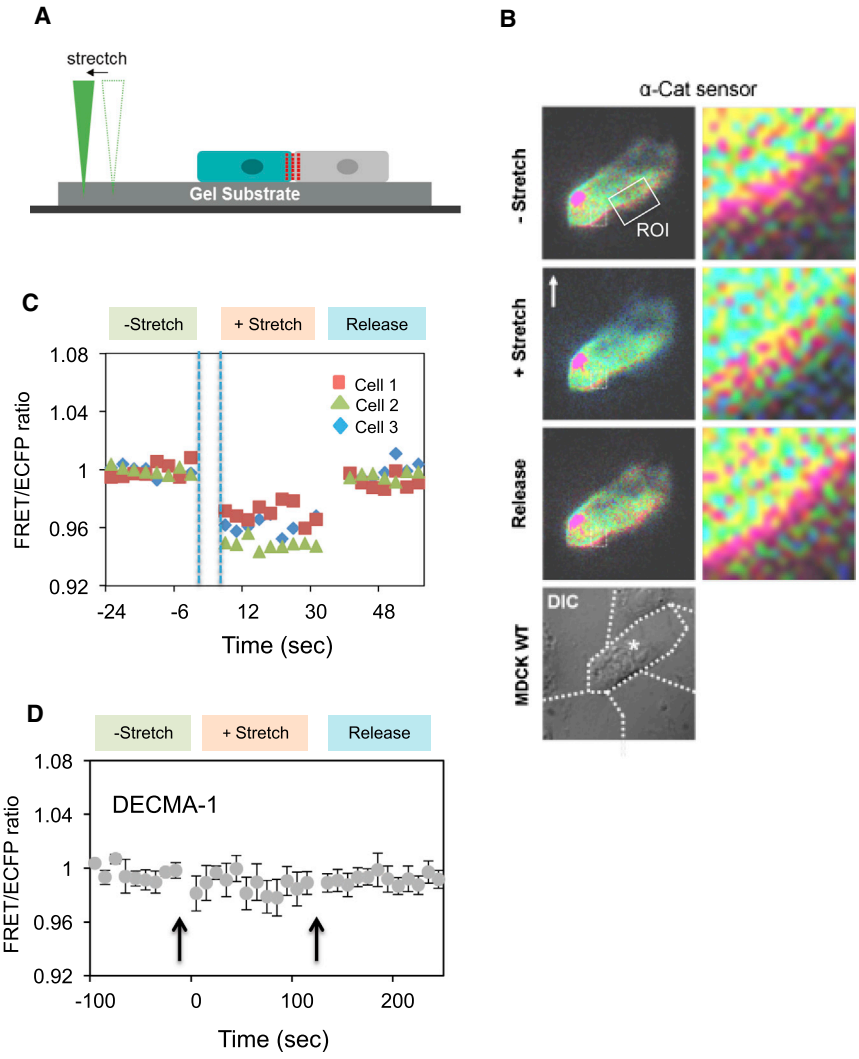

Figure 3. Exogneous Mechanical Stretch Induces Abrupt, Reversible α-Catenin Conformation Switching at Intercellular Junctions

(A) Schematic of the stretching device used to mechanically perturb MDCK WT cells seeded on PA gels (20 kPa) coated with fibronectin.

(B) FRET/ECFP images monitored after substrate stretch and release by the probe, with the direction of the pull relative to the cell indicated by the white arrow. The box indicates the ROI at the junction. The bright red spot in the FRET/ECFP image is a dust particle.

(C) FRET/ECFP ratio versus time before, during, and after release of substrate strain. Data were obtained with MDCK WT cells transiently transfected with the sensor. Time points were taken with a 3 s delay between nanoprobe stretch/release and fluorescence imaging. All three cells exhibited similar behavior after substrate stretch and release.

(D) Effect of the E-cadherin blocking antibody DECMA-1 on the FRET/ECFP ratio versus time during stretch/release cycles. Error bars indicate the SEM.

See also Figure S4.

1.5 s intervals. This rapid response is characteristic of mechanical activation [26, 27].

Within 2 min of force loading, vinculin accumulation was apparent around E-Cad-Fc beads on MDCK WT cells expressing the sensor (Figures 2C and 2D). The force-dependent conformation switch and coincident vinculin recruitment was E-cadherin specific: twisting control poly-L-lysine (PLL) beads neither changed the FRET/ECFP ratio at beads (PLL bead [n = 4] versus E-Cad bead [n = 8], *p < 0.05; Figure 2D) nor triggered vinculin recruitment (Figures 2C and 2D; n = 21–24; E-Cad bead versus PLL bead, ***p < 0.001). These results agree with reports of MDCK KD and DLD1-R2/7 cells rescued with WT α-catenin-GFP [16].

The GFP expressed in MDCK KD cells as a knockdown reporter [28] interferes with sensor imaging (particularly YPet signals) in MTC/FRET measurements. To establish whether the sensor recruits vinculin in a force-dependent manner that requires the VBS, we instead used DLD1-R2/7 cells transfected with the WT sensor or the α-Cat-ΔVBS sensor, which lacks the VBS (Figure 1B). More vinculin accumulated at sheared E-Cad-Fc beads bound to DLD1-R2/7 cells expressing the WT α-Cat sensor (n = 28–36; ***p < 0.001) than to cells expressing the α-Cat-ΔVBS mutant (Figures 2E and 2F). CytoD treatment ablated the force-dependent vinculin accumulation at E-Cad-beads on DLD1-R2/7 cells expressing the sensor (n = 24–36; ***p < 0.001; Figure 2F). These combined MTC/FRET measurements thus demonstrate that the α-catenin sensor undergoes a rapid conformation change in response to E-cadherin-specific mechanical perturbations and that both the sensor and WT α-catenin require the VBS for force-dependent vinculin recruitment [1, 14–16].

Acute External Stretch Triggers Conformation Switching in the Full-Length α-Catenin Sensor

In combined MTC/FRET studies, the decrease in the FRET/ECFP ratio during continuous bead twisting could be due to slower adaptive biochemical signals or to accumulating stretched α-catenin conformers. We tested this by imaging dynamic FRET/ECFP changes at junctions between MDCK WT cells expressing the sensor (Figure 3B) after applying an abrupt step change in junctional tension, using a nanoprobe that stretched the elastomeric cell substrates (Figure 3A). Pressing the probe tip into exposed hydrogel adjacent to cells avoided direct contact with cells. Upon substrate stretch, the FRET/ECFP ratio at junctions decreased abruptly by ~4% to a stable level (Figures 3B and 3C), without further adaptation. After tension release, the signal recoiled immediately to the initial value, with no hysteresis. In these measurements, 3 s was the shortest interval between stretching and FRET imaging (Figure 3C). Measurements at 10 s intervals gave similar results (Figure S4D). Pretreatment with $GdCl_3$ prior to stretch loading had no effect and ruled out contributions from stretch-activated Ca^{2+} channels (data not shown). Cadherin inactivation with blocking DECMA-1 antibody ablated the response (Figure 3D). This immediate, reversible switching suggests that α-catenin functions like an elastic "spring" in series with the cytoskeleton, which deforms with the extracellular matrix and substrate. Comparison of the nanoprobe and MTC measurements indicates that the FRET/ECFP decrease during

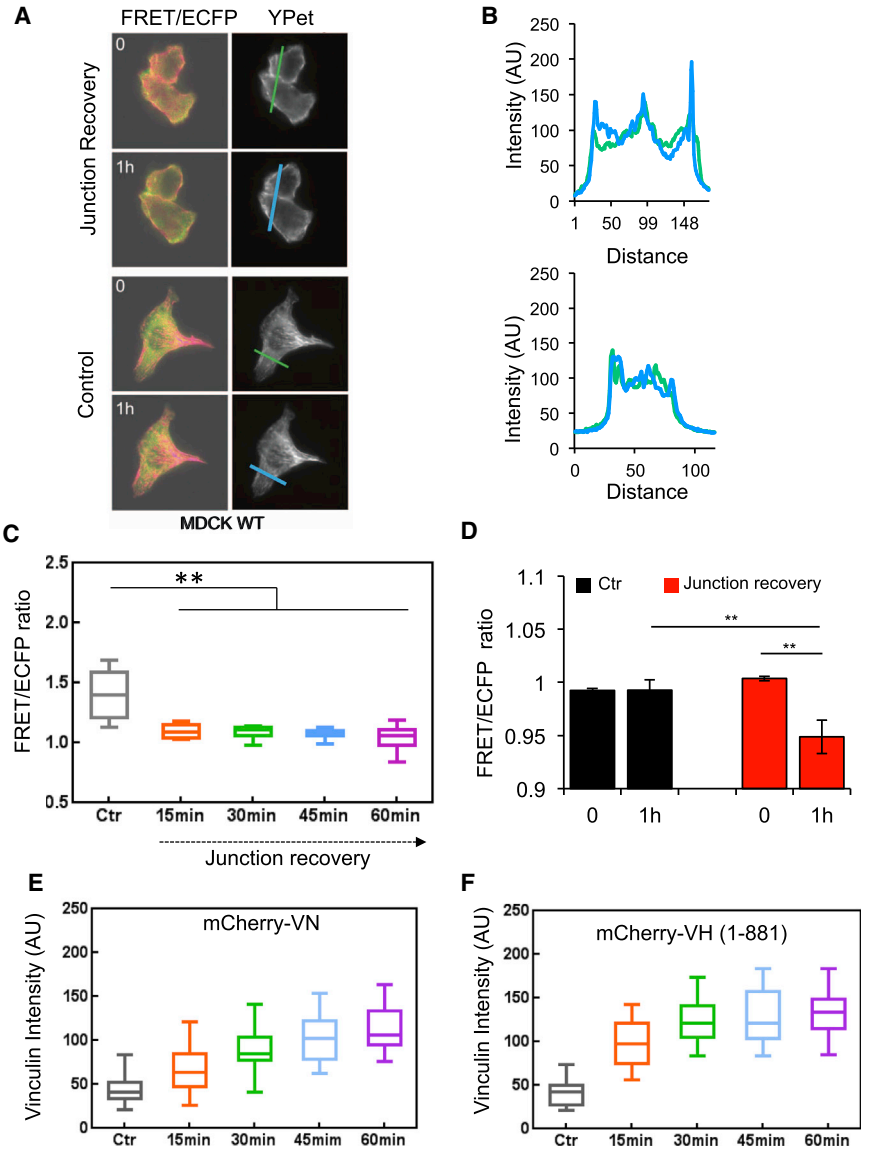

Figure 4. Dynamics of α-Catenin Conformation Switching and Vinculin Recruitment during Junction Recovery after a Calcium Switch

(A) FRET/ECFP and YPet fluorescence images initially and 1 hr after activation of cadherin adhesive function with 2 mM Ca^{2+}. Images of unstimulated control cells are in the lower panels.

(B) Line-scan analyses of the YPet intensity at the indicated junctions (left) of Ca^{2+}-treated (top) and control cells (bottom) during junction recovery. Line scans were at 0 hr (green line) and 1 hr (blue line). In treated cells (top), the decreased FRET/ECFP ratio coincides with an increase in total YPet intensity due to sensor accumulation at the junctions.

(C) FRET/ECFP ratio versus time after calcium addition (n = 9–10).

(D) Bar graphs of the FRET/ECFP ratios before and 1 hr after Ca^{2+} addition (red bars) and in untreated control cells (black bars). After 1 hr, the decreased FRET/ECFP ratio indicates α-catenin conformation switching at reannealing junctions (n = 6; **p < 0.01).

(E) Time dependence of the background-subtracted mCherry-VN fluorescence at ROIs at junctions after calcium addition (n = 31–36).

(F) Background-subtracted mCherry VH (1–881) fluorescence at junctions versus time after calcium addition (n = 31–35).

In (C)–(F), error bars indicate the SEM. See also Figure S3.

bead twisting (Figure 2B) is due to continuous, mechanical perturbation rather than biochemical adaptation.

Biochemical signals during the 3 s interval between substrate stretch and imaging could alter α-catenin. However, the rapid, reversible conformation switching without hysteresis (Figures 3C and S4D) is a signature of mechanical activation and is distinct from slower, dissipative biochemical reactions [26, 27]. By comparison, in PECAM-1 mechanotransduction studies, force-activated adaptive stiffening involves biochemical signaling cascades. Adaptive stiffening had not stabilized 5 s after initial PECAM-1 bead pulls [29]. After releasing tension, a much slower relaxation back to the initial state exhibited hysteresis typical of dissipative biochemical processes [29]. Consequently, the observed rapid, reversible, mechanically triggered conformation switching supports a model in which α-catenin functions as a reversible, elastic force transducer in series with cadherin and actin. Mechanically induced α-catenin unfolding was demonstrated in vitro [30], but these results reveal force actuated, reversible conformation switching and the associated dynamics in live cells. The rapid mechanical response and studies with domain deletion mutants also supports mechanical connectivity between cadherin, α-catenin, and the cytoskeleton.

Studies with two sensor mutants lacking either residues 48–163 or residues 849–906 (Figure 1B) demonstrated that sensor localization to cadherin complexes is required for conformation switching. These deletions removed the β-catenin (Δβ-catenin) or F-actin (ΔF-actin) binding sites, respectively. The Δβ-catenin mutant cannot bind the cadherin/β-catenin complex and did not localize to junctions (Figure S4E). Consistent with previous reports [14, 31, 32], the ΔF-actin mutant also remained in the cytoplasm, without clear junctional localization (Figure S4E). The latter behavior may be due to the adoption of a conformation that allosterically impedes binding to β-catenin at junctions [14, 33]. In MDCK WT cells, neither of these constructs exhibited stretch-dependent changes in FRET/ECFP ratios, either at junctions or in the cytosol (Figure S4F). CytoD treatment also did not alter FRET signals in MDCK KD cells expressing either of these truncated sensors (Figures S4E and S4F).

Force-Activated Vinculin Recruitment to Intercellular Junctions Lags α-Catenin Conformation Switching

The dynamics of α-catenin conformation switching and vinculin recruitment in live cells were quantified during junction recovery, after a calcium switch. In line scans of cell-cell junctions (Figures 4A and 4B) 1 hr after reactivation of cadherins with 2mM Ca^{2+}, the YPet intensity increased due to sensor accumulation at the reannealing junctions (Figures 4A and B). This coincided with a temporal decrease in FRET/ECFP

ratios at junctions (Figures 4C and 4D). There was no change in control cells without Ca^{2+} (Figures 4A, 4B, and 4D). The α-catenin conformation switching dynamics were slower during junction recovery (Figures 4C and 4E) than after Ca^{2+} removal (Figure S2B). The switching rate during junction recovery, estimated from a weighted nonlinear least-squares fit of the FRET/ECFP decay (Figure 4E) to a first order rate equation (Supplemental Information), was 0.15 ± 0.06 min^{-1}.

The postulated vinculin coactivation by α-catenin and actin [34] suggested that α-catenin conformation switching might precede force-dependent vinculin accumulation at junctions. Immunofluorescence imaging showed that vinculin accumulates at reannealing adhesions after Ca^{2+} activation [21]. Figure 4E shows the vinculin recruitment dynamics, quantified from fluorescence images of mCherry vinculin in ROIs at reannealing junctions. The FRET/ECFP ratio decreased to the near steady-state level within 15 min (n = 9–10; **p < 0.01, relative to control) (Figure 4C), but vincullin accumulated more slowly during the 60 min observation period (n = 32–36; **p < 0.01) (Figure 4E). The accumulation rate, estimated by fitting the vinculin accumulation time course (Figure 4E) to pseudo first-order kinetics, was 0.025 ± 0.002 min^{-1}. Immunofluorescence imaging (Figure S3C) gave similar results: 0.017 ± 0.004 min^{-1}. Thus, vinculin recruitment continues long after the α-catenin conformation reaches steady state at resealing junctions (Figure 4E), and after 2 min of E-cadherin bead twisting (data not shown). Although vinculin could also bind β-catenin [35], it did not accumulate at reannealing junctions between DLD1-R2/7 cells expressing the α-Cat-ΔVBS-GFP sensor (Figure S3C). Therefore, in cells used in this study, vinculin accumulation requires α-catenin and its VBS, and the kinetics reflect vinculin recruitment to activated α-catenin. Whether vinculin recruitment also requires F-actin binding remains to be established.

Comparison of the recruitment dynamics of vinculin with mCherry-labeled, constitutively active vinculin head domain (VH, residues 1–881; Figure 4F) demonstrated that the slow vinculin accumulation kinetics is due to its slow autoinhibition release [36]. The fitted mCherry VH accumulation rate of 0.06 ± 0.01 min^{-1} was 3.5-fold faster than that of full-length mCherry VN. Although the mCherry VH expression was slightly higher than mCherry VN, it would need to be at least four times higher in order for concentration differences to account for the different kinetics. Similarly, despite the immediate α-catenin conformation switch at junctions between briefly stretched (<2 min) MDCK monolayers, mCherry VH accumulation was slower, requiring several minutes of sustained stretch before statistically significant increases in mCherry VH were detected (Figure S3D). Once docked, mCherry VH was retained for at least 10 min after tension release (Figures S3D and S3E). The slow release is consistent with the 98 ± 19 nM dissociation constant between α-catenin and the vinculin head domain [37] that could kinetically stabilize the complex. Together, these findings directly demonstrate that, in live cells, the force activation of α-catenin and vinculin recruitment occur sequentially, rather than by a concerted mechanism.

In summary, our engineered FRET-based α-catenin conformation sensor localizes to cadherin complexes at intercellular junctions and restores α-catenin dependent adhesive functions. This sensor undergoes immediate, reversible α-catenin conformation switching at cadherin adhesions in response to mechanical perturbations. These results support the postulate that α-catenin is an elastic, mechanically activated force transducer in series with cadherin and the cytoskeleton [1]. Kinetic analyses of coordinated conformation switching dynamics and vinculin recruitment further exposed molecular cascades in cadherin-based force transduction. Future comparisons of α-catenin sensor dynamics with force-dependent biochemical changes will uniquely reveal coordinated mechanical and biochemical events during mechanotransduction in live cells with high spatiotemporal resolution.

Experimental Procedures

Complete experimental procedures are provided in the Supplemental Experimental Procedures.

Reagents and Cells

The α-catenin conformation sensor was engineered by inserting the ECFP and acceptor YPet at the N- and C-terminal regions flanking the central force-sensing core of α-catenin (domains D2–D4). Five additional mutants were engineered for controls.

The following cell types were transiently transfected with the α-catenin sensor or its mutants: wild-type Madine Darby canine kidney (MDCK WT) cells, an α-catenin knockdown MDCK line (MDCK KD; a gift from J. Nelson, Stanford [28]), DLD1 cells, and DLD1-R2/7, which is an α-catenin null subclone of the DLD1 line [38].

Vinculin recruitment was visualized with mCherry-vinculin (mCherry VN; from J. de Rooij, Utrecht) or by immunofluorescence imaging. Constitutively active mCherry (mCherry-VH, 1–881) was engineered as described in the Supplemental Experimental Procedures.

Junction Disruption

Tension across cadherin-based cell-cell junctions was disrupted by treatment of cells with the cadherin-blocking antibody DECMA-1, by inactivation of cadherin via Ca^{2+} depletion, or by disruption of actin with cytochalasin D treatment.

Junction Reannealing after Calcium Switching

The addition of 2 mM calcium after junction disruption activated cadherins and the subsequent restoration of cell-cell adhesions and junctional tension.

Time-Lapse Live-Cell Imaging

Live-cell fluorescent images were obtained with a Zeiss Axiovert 200 inverted microscope and MetaFluor 6.2 software (Universal Imaging). The emission ratios of YPet/ECFP (referred to as the FRET/ECFP ratio) were directly computed using MetaFluor software and were further analyzed with Excel (Microsoft). During junction recovery assays, images were acquired with a Nikon fluorescence microscope with the Perfect Focus System, and image acquisition and analysis were performed with MetaFluor 7.6 software.

Combined MTC and FRET

Magnetic beads coated with E-cadherin extracellular domains attached to cadherin receptors on the cell surface. An oscillating magnetic field twists the beads to generate shear stress on E-cadherin bonds. FRET/ECFP ratios in ROIs around the sheared beads (combined MTC/FRET) visualized force-activated changes in the sensor conformation triggered by mechanical perturbation of specific E-cadherin bonds.

Substrate Stretching Measurements

Cells were cultured on an elastomeric substrate, and a nanoprobe was pressed into the substrate near the cells (Figure 3A). Tangential pulling of the probe stretched the substrate together with the extracellular matrix and attached cells to increase tension across the cell-cell contacts.

Statistical Analysis

The fluorescence imaging and traction force results were expressed as the mean and SEM. The statistical significance of differences between two mean values was assessed using a Welch's t test or ANOVA supported by GraphPad Prism 6.0 software. A statistically significant difference at the 95% confidence level is defined by a p value <0.05.

Supplemental Information

Supplemental Information includes Supplemental Experimental Procedures and four figures and can be found with this article online at http://dx.doi.org/10.1016/j.cub.2014.11.017.

Author Contributions

T.-J.K. conceived and designed the study, performed experiments, analyzed and interpreted the data, wrote the manuscript, and gave final approval of manuscript. S.Z. conceived and designed the study, performed experiments, and wrote the manuscript. J.S. conceived and designed the study and performed experiments. L.L., J.W., X.K., and I.M.: conceived the study and performed experiments. D.E.L and Y.W.; conceived and designed the study, analyzed and interpreted the data, wrote the manuscript, and gave final approval of manuscript.

Acknowledgments

This work was supported in part by grants NIH HL098472, NIH HL109142, NSF CBET 08-46429 (Y.W.), NIH 1 R01 GM097443 (D.E.L.), and NSF CBET 11-32116 (D.E.L. and Y.W.). We thank N. Wang for use of the magnetic twisting cytometer.

Received: April 7, 2014
Revised: September 26, 2014
Accepted: November 6, 2014
Published: December 24, 2014

References

1. Yonemura, S., Wada, Y., Watanabe, T., Nagafuchi, A., and Shibata, M. (2010). alpha-Catenin as a tension transducer that induces adherens junction development. Nat. Cell Biol. *12*, 533–542.
2. Lecuit, T., Lenne, P.F., and Munro, E. (2011). Force generation, transmission, and integration during cell and tissue morphogenesis. Annu. Rev. Cell Dev. Biol. *27*, 157–184.
3. Huveneers, S., and de Rooij, J. (2013). Mechanosensitive systems at the cadherin-F-actin interface. J. Cell Sci. *126*, 403–413.
4. Leckband, D., and de Rooij, J. (2014). Cadherin adhesion and mechanosensing. Annu. Rev. Cell Dev. Biol. *30*, 291–315.
5. Rauzi, M., Lenne, P.F., and Lecuit, T. (2010). Planar polarized actomyosin contractile flows control epithelial junction remodelling. Nature *468*, 1110–1114.
6. Diz-Muñoz, A., Krieg, M., Bergert, M., Ibarlucea-Benitez, I., Muller, D.J., Paluch, E., and Heisenberg, C.P. (2010). Control of directed cell migration in vivo by membrane-to-cortex attachment. PLoS Biol. *8*, e1000544.
7. Papusheva, E., and Heisenberg, C.P. (2010). Spatial organization of adhesion: force-dependent regulation and function in tissue morphogenesis. EMBO J. *29*, 2753–2768.
8. Maître, J.L., Berthoumieux, H., Krens, S.F., Salbreux, G., Jülicher, F., Paluch, E., and Heisenberg, C.P. (2012). Adhesion functions in cell sorting by mechanically coupling the cortices of adhering cells. Science *338*, 253–256.
9. Leerberg, J.M., Gomez, G.A., Verma, S., Moussa, E.J., Wu, S.K., Priya, R., Hoffman, B.D., Grashoff, C., Schwartz, M.A., and Yap, A.S. (2014). Tension-sensitive actin assembly supports contractility at the epithelial zonula adherens. Curr. Biol. *24*, 1689–1699.
10. Fernandez-Gonzalez, R., Simoes, Sde.M., Röper, J.C., Eaton, S., and Zallen, J.A. (2009). Myosin II dynamics are regulated by tension in intercalating cells. Dev. Cell *17*, 736–743.
11. Na, S., and Wang, N. (2008). Application of fluorescence resonance energy transfer and magnetic twisting cytometry to quantify mechanochemical signaling activities in a living cell. Sci. Signal. *1*, pl1.
12. Taguchi, K., Ishiuchi, T., and Takeichi, M. (2011). Mechanosensitive EPLIN-dependent remodeling of adherens junctions regulates epithelial reshaping. J. Cell Biol. *194*, 643–656.
13. Huveneers, S., Oldenburg, J., Spanjaard, E., van der Krogt, G., Grigoriev, I., Akhmanova, A., Rehmann, H., and de Rooij, J. (2012). Vinculin associates with endothelial VE-cadherin junctions to control force-dependent remodeling. J. Cell Biol. *196*, 641–652.
14. Thomas, W.A., Boscher, C., Chu, Y.S., Cuvelier, D., Martinez-Rico, C., Seddiki, R., Heysch, J., Ladoux, B., Thiery, J.P., Mege, R.M., and Dufour, S. (2013). α-Catenin and vinculin cooperate to promote high E-cadherin-based adhesion strength. J. Biol. Chem. *288*, 4957–4969.
15. Twiss, F., Le Duc, Q., Van Der Horst, S., Tabdili, H., Van Der Krogt, G., Wang, N., Rehmann, H., Huveneers, S., Leckband, D.E., and De Rooij, J. (2012). Vinculin-dependent Cadherin mechanosensing regulates efficient epithelial barrier formation. Biol. Open *1*, 1128–1140.
16. Barry, A.K., Tabdili, H., Muhamed, I., Wu, J., Shashikanth, N., Gomez, G.A., Yap, A.S., Gottardi, C.J., de Rooij, J., Wang, N., and Leckband, D.E. (2014). α-catenin cytomechanics—role in cadherin-dependent adhesion and mechanotransduction. J. Cell Sci. *127*, 1779–1791.
17. Ladoux, B., Anon, E., Lambert, M., Rabodzey, A., Hersen, P., Buguin, A., Silberzan, P., and Mège, R.M. (2010). Strength dependence of cadherin-mediated adhesions. Biophys. J. *98*, 534–542.
18. Geiger, B., Spatz, J.P., and Bershadsky, A.D. (2009). Environmental sensing through focal adhesions. Nat. Rev. Mol. Cell Biol. *10*, 21–33.
19. Ozawa, M., Hoschützky, H., Herrenknecht, K., and Kemler, R. (1990). A possible new adhesive site in the cell-adhesion molecule uvomorulin. Mech. Dev. *33*, 49–56.
20. Maruthamuthu, V., Sabass, B., Schwarz, U.S., and Gardel, M.L. (2011). Cell-ECM traction force modulates endogenous tension at cell-cell contacts. Proc. Natl. Acad. Sci. USA *108*, 4708–4713.
21. le Duc, Q., Shi, Q., Blonk, I., Sonnenberg, A., Wang, N., Leckband, D., and de Rooij, J. (2010). Vinculin potentiates E-cadherin mechanosensing and is recruited to actin-anchored sites within adherens junctions in a myosin II-dependent manner. J. Cell Biol. *189*, 1107–1115.
22. Drees, F., Pokutta, S., Yamada, S., Nelson, W.J., and Weis, W.I. (2005). Alpha-catenin is a molecular switch that binds E-cadherin-beta-catenin and regulates actin-filament assembly. Cell *123*, 903–915.
23. Piljić, A., de Diego, I., Wilmanns, M., and Schultz, C. (2011). Rapid development of genetically encoded FRET reporters. ACS Chem. Biol. *6*, 685–691.
24. Sun, Y., Wang, X., Yuan, S., Dang, M., Li, X., Zhang, X.C., and Rao, Z. (2013). An open conformation determined by a structural switch for 2A protease from coxsackievirus A16. Protein Cell *4*, 782–792.
25. Tabdili, H., Langer, M., Shi, Q., Poh, Y.-C., Wang, N., and Leckband, D. (2012). Cadherin-dependent mechanotransduction depends on ligand identity but not affinity. J. Cell Sci. *125*, 4362–4371.
26. Weber, G.F., Bjerke, M.A., and DeSimone, D.W. (2012). A mechanoresponsive cadherin-keratin complex directs polarized protrusive behavior and collective cell migration. Dev. Cell *22*, 104–115.
27. Na, S., Collin, O., Chowdhury, F., Tay, B., Ouyang, M., Wang, Y., and Wang, N. (2008). Rapid signal transduction in living cells is a unique feature of mechanotransduction. Proc. Natl. Acad. Sci. USA *105*, 6626–6631.
28. Benjamin, J.M., Kwiatkowski, A.V., Yang, C., Korobova, F., Pokutta, S., Svitkina, T., Weis, W.I., and Nelson, W.J. (2010). AlphaE-catenin regulates actin dynamics independently of cadherin-mediated cell-cell adhesion. J. Cell Biol. *189*, 339–352.
29. Collins, C., Guilluy, C., Welch, C., O'Brien, E.T., Hahn, K., Superfine, R., Burridge, K., and Tzima, E. (2012). Localized tensional forces on PECAM-1 elicit a global mechanotransduction response via the integrin-RhoA pathway. Curr. Biol. *22*, 2087–2094.
30. Yao, M., Qiu, W., Liu, R., Efremov, A.K., Cong, P., Seddiki, R., Payre, M., Lim, C.T., Ladoux, B., Mège, R.M., and Yan, J. (2014). Force-dependent conformational switch of α-catenin controls vinculin binding. Nat. Commun. *5*, 4525.
31. Desai, R., Sarpal, R., Ishiyama, N., Pellikka, M., Ikura, M., and Tepass, U. (2013). Monomeric α-catenin links cadherin to the actin cytoskeleton. Nat. Cell Biol. *15*, 261–273.
32. Pappas, D.J., and Rimm, D.L. (2006). Direct interaction of the C-terminal domain of alpha-catenin and F-actin is necessary for stabilized cell-cell adhesion. Cell Commun. Adhes. *13*, 151–170.
33. Rangarajan, E.S., and Izard, T. (2013). Dimer asymmetry defines α-catenin interactions. Nat. Struct. Mol. Biol. *20*, 188–193.
34. Kwiatkowski, A.V., Maiden, S.L., Pokutta, S., Choi, H.J., Benjamin, J.M., Lynch, A.M., Nelson, W.J., Weis, W.I., and Hardin, J. (2010). In vitro and in vivo reconstitution of the cadherin-catenin-actin complex from Caenorhabditis elegans. Proc. Natl. Acad. Sci. USA *107*, 14591–14596.
35. Peng, X., Cuff, L.E., Lawton, C.D., and DeMali, K.A. (2010). Vinculin regulates cell-surface E-cadherin expression by binding to beta-catenin. J. Cell Sci. *123*, 567–577.
36. Ziegler, W.H., Liddington, R.C., and Critchley, D.R. (2006). The structure and regulation of vinculin. Trends Cell Biol. *16*, 453–460.
37. Peng, X., Maiers, J.L., Choudhury, D., Craig, S.W., and DeMali, K.A. (2012). α-Catenin uses a novel mechanism to activate vinculin. J. Biol. Chem. *287*, 7728–7737.
38. Vermeulen, S.J., Bruyneel, E.A., Bracke, M.E., De Bruyne, G.K., Vennekens, K.M., Vleminckx, K.L., Berx, G.J., van Roy, F.M., and Mareel, M.M. (1995). Transition from the noninvasive to the invasive phenotype and loss of alpha-catenin in human colon cancer cells. Cancer Res. *55*, 4722–4728.